An integrative approach to understanding pyrethroid resistance in *Rhipicephalus microplus* and *R. decoloratus* ticks

Roelof DJ van Wyk[1*], Samantha Baron[2*], Christine Maritz Olivier[2#]

[1]Department of Biochemistry, University of Pretoria, Pretoria, South Africa
[2]Department of Genetics, University of Pretoria, Pretoria, South Africa

*Authors contributed equally

[#]Corresponding author**:** Christine Maritz-Olivier, Tel: +27 (012) 420 3945. Fax: +27 (012) 362 5327. Postal address: 8th Floor, Agricultural Sciences Building, University of Pretoria, Hatfield, Pretoria, 0083, South Africa. Email: Christine.maritz@up.ac.za

Abstract

Rhipicephalus microplus and *Rhipicephalus decoloratus* species occur in regions with savannah and temperate climates, typically in grassland and wooded areas used as cattle pasture. Both species are associated with the transmission of *Anaplasma* and *Babesia* spp., impacting livestock health and quality of livestock-associated products. In Africa, tick control is predominantly mediated with the use of acaricides, such as synthetic pyrethroids. After several years on the market, reports of resistance to synthetic pyrethroids escalated but limited field data and validation studies have been conducted to determine the extent of acaricide resistance in Africa. Without this data, knowledge-based tick control will remain problematic and selection pressure will remain high increasing the rate of resistance acquisition.

To date, several pyrethroid resistance associated single nucleotide polymorphisms (SNPs) have been reported for arthropods within the voltage-gated sodium channel. Three SNPs have been identified within this channel in pyrethroid resistant *R. microplus* ticks, but none has been reported for *R. decoloratus*. This study is the first to report the presence of a shared SNP within the voltage-gated sodium channel in both *R. microplus* and *R. decoloratus*, which is directly linked to pyrethroid resistance in *R. microplus*. As the mode of action by which these SNPs mediate pyrethroid resistance remains unknown, this study aims to set hypotheses by means of predictive structural modelling. This not only paves the way forward to elucidating the underlying biological mechanisms involved in pyrethroid resistance, but also improvement of existing acaricides and ultimately sustainable tick control management.

Keywords: *Rhipicephalus microplus*, *Rhipicephalus decoloratus*, pyrethroids, acaricide resistance, SNPs, protein modelling, drug docking

Introduction

Rhipicephalus microplus and *Rhipicephalus decoloratus* ticks are widely distributed in suitable habitats throughout Africa, south of the Sahara. These species often occur together with *R. annulatus* and *R. geigyi* and are associated with the spread of babesiosis and anaplasmosis to cattle (Walker et al., 2003). *R. microplus* is well known for the detrimental socio-economic impact it inflicts on the cattle industry in terms of beef and dairy production (Jonsson, 2006; Jonsson et al., 2001).

The foremost tick control strategy implemented by farmers in South Africa, and most of southern Africa, is the use of chemical acaricides. The main concern at this point is the declining efficacy of current acaricides due to the development of resistance. Resistance to organophosphates (OPs) first came about in the 1980's (Aguirre et al., 1986) after which synthetic pyrethroids and amitraz were introduced to circumvent organophosphate-resistant ticks (Aguirre et al., 1986; Vargas et al., 2002). This led to the extensive use of synthetic pyrethroids and consequently the prevalent eruption of pyrethroid resistance in the 1990's (He et al., 1999; Miller et al., 1999).

Metabolic resistance towards pyrethroids has been documented in the Coatzacoalcos Mexican *R. microplus* tick strain based on synergistic assays with piperonyl butoxide (PBO) and triphenyl phosphate (TPP) (Miller et al., 1999). Within this particular strain, there was also an up-regulation in the expression of an esterase (CzEst9) predicted to be involved in the rapid hydrolysis of permethrin (Pruett et al., 2002). Subsequent studies confirmed that this carboxylesterase enzyme played a key role in pyrethroid resistance in the Mato Grosso Brazilian strain (Baffi et al., 2007).

Three single nucleotide polymorphisms (SNPs) in the voltage-gated sodium channel have been reported to be associated with pyrethroid resistance in ticks, evidently indicating that target site resistance is the most prevalent resistance mechanism against pyrethroids in *R. microplus* ticks. The first SNP was discovered in domain III of the sodium channel in pyrethroid resistant tick populations from Mexico, and was also reported to be confined to North America (Guerrero et al., 2012; He et al., 1999). Target site mutations resulting in pyrethroid resistance were predominantly

found to occur in domain II of the voltage-gated sodium channel in a number of other arthropods that were investigated (Soderlund and Knipple, 2003). This subsequently led to the discovery of two SNPs in domain II segments 4-5 (DIIS4-S5) of the linker region of the sodium channel in *R. microplus* (Jonsson et al., 2010; Morgan et al., 2009). Of the three reported mutations it has been shown that the one described by Morgan et al. (2009) occurs in South African *R. microplus* ticks (Guerrero et al., 2012). No pyrethroid resistance associated mutations have been reported in the sodium channel for *R. decoloratus*.

A step towards understanding the impact of these SNPs on the structure and biological function of the voltage-gated sodium channel is through *in silico* predictive modelling. To date only 58 crystal structures are available (according to RCSB PDB database) for voltage-gated sodium channels, with most of the structures only partially resolved.

Previous attempts to construct a model for the *R. microplus* voltage-gated sodium channel utilised an existing housefly model, constructed from several voltage-gated potassium channel template structures with only a few corresponding amino acid substitutions (O' Reilly et al., 2014). Research by O'Reilly et al. (2014) illustrated a pyrethroid resistance-associated SNP (position F1519I) that occurred in the S6 transmembrane helix of domain III. This does not correspond to the most prevalent SNP marker (position L64I) that occurs in domain II, which has been documented in both Mexico and Brazil as a viable resistance marker (Guerrero et al., 2012). To date, only the domain II S4-S5 linker region marker has been observed globally for pyrethroid resistant *R. microplus* ticks.

The model proposed in this study focuses on the L64I marker and therefore contributes insight to resistance mediated by domain II. The study by O'Reilly et al. (2014) and colleagues was used as criteria for determining relevant docked poses for cypermethrin, however the amino acid sequence identity for the housefly model with the corresponding crystal templates was below 30%. Therefore, we set out to construct a higher quality model with higher sequence coverage in amino acid sequence alignments.

Insight into the status of pyrethroid resistance within South Africa will aid in the development of improved tick control strategies in the hope of prolonging the use of current acaricides. With increased selection pressure promoting the development of acaricide resistance, the progression towards novel control strategies is more imperative than ever before.

Methods and materials:

Tick Collection, identification and DNA extraction

Ticks were collected by representatives of Zoetis South Africa (Pty) Ltd. from108 farms across South Africa, including Swaziland with written consent from each farmer. Collection points are shown in Figure S1. Ticks were sorted into genera according to published guidelines (Madder and Horak, 2010; Walker et al., 2003). Distinction between *Rhipicephalus* species was done using microscopy to evaluate hypostome dentition and adanal spur features (Madder and Horak, 2010; Walker et al., 2003). Morphology results were validated through molecular identification using restriction fragment length polymorphism (RFLP) analysis (Lempereur et al., 2010). A salt based extraction protocol was used for genomic DNA extraction from individual adult ticks (Baron et al., 2015). A full repository of all ticks used in this study is shown in Table S1 and S2.

PCR amplification of *R. microplus* voltage-gated sodium channel gene fragment

Published primers were used to amplify a fragment of domain II segment 4-5 region of the sodium channel (Morgan et al., 2009). Each reaction contained 200 ng of gDNA template, 10 pmol of each primer and KAPA2G™ Robust HotStart ReadyMix (200 µM dNTPs, 2.0 mM $MgCl_2$) in a final 25 µl reaction. The cycling parameters were as follows; 94°C for 4 min, followed by 40 cycles of 94°C for 30 s, 51°C for 30 s and 72°C for 1 min with a final extension at 72°C for 7 min.

Allele-specific PCR for the voltage-gated sodium channel of *R. decoloratus*

Allele-specific PCR of *R. decoloratus* voltage-gated sodium channel was conducted using allele-specific primers (Guerrero et al., 2001). This was done in order to reduce

the cost of sequencing and to increase overall productivity. Several samples were sequenced for validation of the amplified PCR products. For each sample two reactions were set up. One reaction containing the susceptible forward primer (5'-GGAAAACCATCGGTGCTC-3': L64IS) and the diagnostic/reverse primer (5'-GAACTTGTGTTTACTTTCTTCGTAGT-3'). The second reaction contained the resistant forward primer (5'-GGAAAACCATCGGTGCTA-3': L64IR) as well as the diagnostic reverse primer. PCR conditions for both susceptible (L64IS) and resistant (L64IR) reactions were as follows: a 25 µl reaction made up using water (SABAX®, ADCOCK-INGRAM), 100 ng gDNA, 10 pmol forward and reverse primer and Econo*Taq*® PLUS GREEN 2X Master Mix. The cycling parameters were 94°C for 4 min, followed by 40 cycles of 94°C for 30 s, 51°C for 30 s and 72°C for 1 min with a final extension at 72°C for 7 min.

Sequencing and analysis of amplified PCR products

PCR products were sequenced by Macrogen Inc. (Netherlands). Individual chromatograms were manually curated using BioEdit sequence alignment editor version 7.2.0 (Hall, 1999). Multiple alignments were constructed using the online MAFFT program version 6 (http://mafft.cbrc.jp/alignment/software/) (Katoh and Standley, 2013) to identify resistance associated mutations. To test for neutrality within DNA sequences, the Tajima D value (Tajima, 1989) was calculated using MEGA5 (Tamura et al., 2011). This test for neutrality was conducted on the multiple sequence alignment to determine if directional or balancing selection was acting on domain II S4-5 linker region of the voltage-gated sodium channel.

Template selection and model construction

Protein BLAST (BLASTp algorithm) was performed for all of the target protein sequences from literature of *R. microplus* against the protein data bank (PDB). Maximum coverage (above 80%) and sequence identities (above 30%) were used as cut off values. Protein crystal structures were obtained from PDB (http://www.rcsb.org/). Pfam seed alignments were included for target protein sequences (http://pfam.sanger.ac.uk/). Multiple-sequence alignments were done for the template and seed alignments using MAFFT version 6. All alignments were performed using the G-INS-i parameter global alignment algorithm (Needleman-Wunsch algorithm) and the BLOSUM62 matrix. The sequence for the voltage-gated

sodium channel of *R. microplus* was used for model building (AF134216.2). Homology models were generated using Modeller 9v1 within the Discovery studio 4.0® suite (Accelrys software Inc, USA). From the template and target sequence alignments, homology models were generated for all proteins sharing a sequence identity of 30% or more with their respective templates. All relevant ligands co-crystallized with the protein structures were included during model building. Energy minimization rounds where applied as per default by the software. Homology protein models were submitted for quality assessment to PDBsum (http://www.ebi.ac.uk/thornton-srv/databases/pdbsum/Generate.html).

Drug docking

Docking of cypermethrin for the *R. microplus* voltage-gated sodium channel (RmvNaCh) model was done using AutoDock vina (Trott and Olson, 2009). Docking spheres for the voltage-gated sodium channel centralized round the resistance SNP site (Morgan et al., 2009) at a radius of 10 Å. Each docking run allowed for flexibility of all side chains in the docking sphere, flexibility of the ligand rotatable bonds and an exhaustiveness of 8. Docking files were assessed using AutoDock tools 1.5.6. Bond interaction of the generated poses and all images for docking results was done using Discovery studio 4.0® suite (Accelrys software Inc, USA). Root mean square deviation (RMSD) of ligand atom distances were calculated using Discovery studio 4.0® suite (Accelrys software Inc, USA). To compare the distance of each of the different stereoisomers in their docked state with one another and relating these docked results based on distances deviated in angstroms Å, the RMSD is calculated by comparing all atoms involved in the docked poses generated for each stereoisomer and systematically comparing these spaces with each other.

Results:

Tick collection

Approximately 40% of the 108 farms sampled were found to be co-infested with both *R. microplus* and *R. decoloratus,* with three most common tick genera being *Amblyomma*, *Hyalomma* and *Rhipicephalus* (results not shown).

Pyrethroid resistance-associated SNP markers present in the voltage-gated sodium channel of *R. microplus* and *R. decoloratus*.

Multiple sequence alignments of the representative sequences identified is shown in Figure 1 with the known pyrethroid resistance associated SNP at nucleotide position 23 (a C to A mutation, L64I) detected in both *R. microplus* and *R. decoloratus*. The homozygous-resistant genotype (AA) predominated in the *R. microplus* population with a frequency of 58.8%, while the homozygous-susceptible genotype (CC) occurred at a frequency of 32.4% (Figure 2). The remainder of the studied tick population (8.8%) was heterozygous (CA) and displayed both the wild-type and susceptible alleles. The latter is supported by a low Tajima D value of -0.372 (<0) indicating a lower average of heterozygosity.

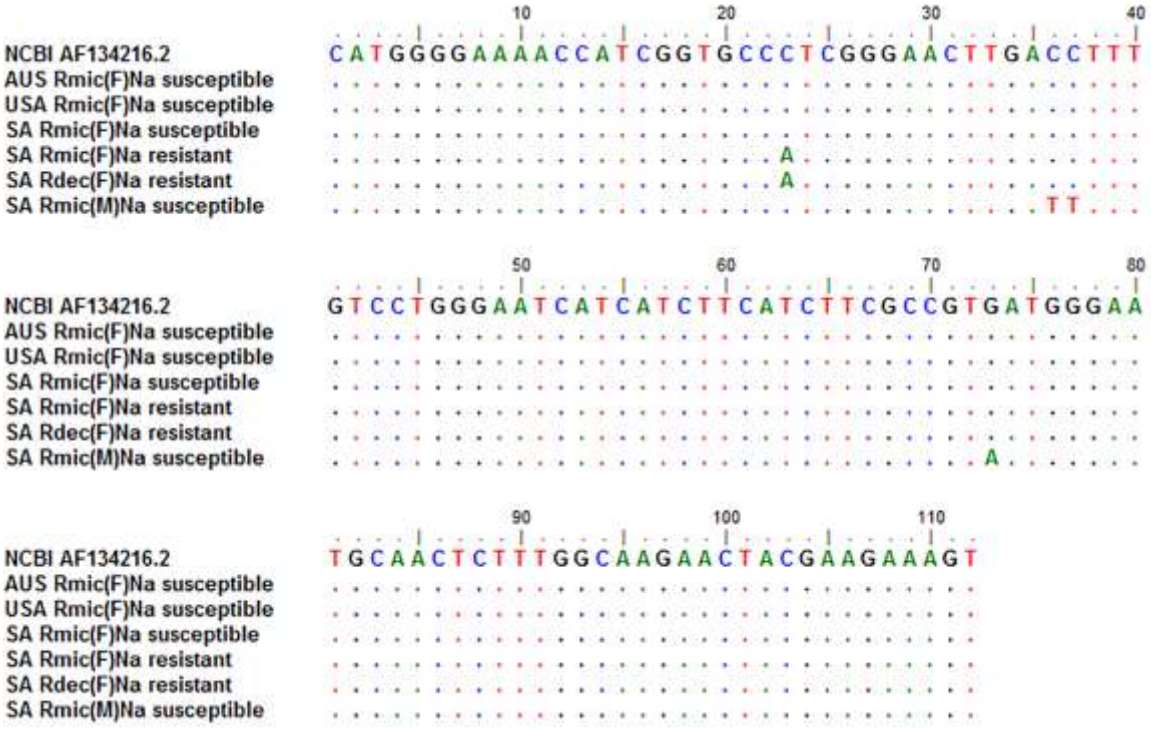

Figure 1: Multiple sequence alignment of the voltage-gated sodium channel of representative sequences from both *R. microplus* and *R. decoloratus* samples. NCBI: AF134216.2 represents the NCBI reference strain with the accession number indicated. Rmic: *R. microplus*, Rdec: *R. decoloratus*, AUS: Australia, USA: America, SA: South Africa, (F): Female ticks, (M): Male ticks, Na: Sodium channel. Samples displaying the C-A mutation at nucleotide position 23 are resistant to pyrethroids as published by Morgan et al., (2009).

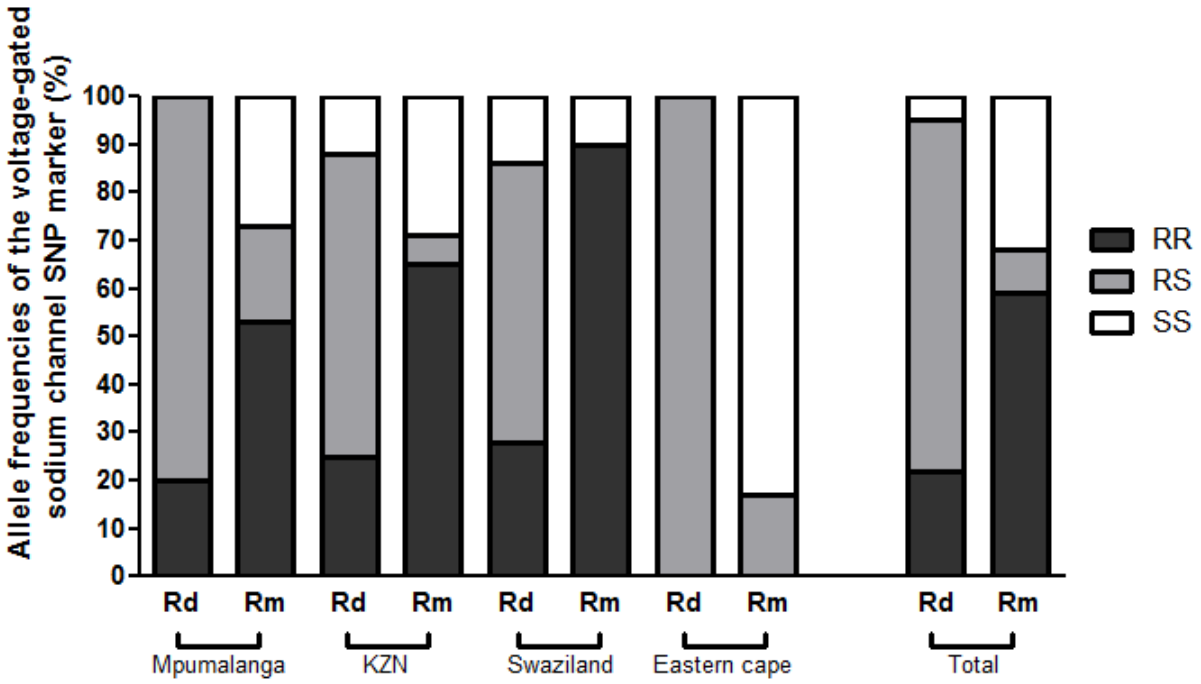

Figure 2: Comparison of pyrethroid resistant alleles in *R. microplus* and *R. decoloratus* populations of South Africa. A staggered bar graph illustrates the ratios of hetero-and homozygosity in the voltage-gated sodium channel for the resistance and susceptible alleles. RR = homozygous-resistant, RS = heterozygous and SS = homozygous-susceptible

No other SNPs were found in domain II S4-5 linker region of the sodium channel from female *R. microplus* field strains. However, the male *R. microplus* tick samples (Figure 1) had three additional mutations within this short segment of the voltage-gated sodium channel. The first two occurred at nucleotide position 36 and 37 within the multiple alignment, and resulted in an amino acid change at position 68 from a threonine to an isoleucine residue (T68I). An additional synonymous mutation was found at nucleotide position 73 (G to A). Although the overall effects of these mutations are not yet known, it might be postulated to have a certain fitness advantage for the male ticks.

Protein models of the voltage-gated sodium channel (RmvNaCh) with cypermethrin interactions

Only a partial model for the voltage-gated sodium channel could be constructed due to incomplete sequence data for *R. microplus* and lack of a high quality crystal structure template. A multiple amino acid sequence alignment of *R. microplus* voltage-gated sodium channel with ticks, mites and insects highlights the specific region constructed during modelling (Figure 3). The amino acid sequence of *R.*

microplus shared only 30.2% identity with the template (4DXW) but included sufficient sequence to allow assessment of cypermethrin binding into the binding pocket. Although the alignment was done in accordance with O'Reilly et al. (2014), a larger section of domain II was included into the RmvNaCh model. The model by O'Reilly et al. (2014) only looked at DIIS4-S5 linker region and up to DIIS5, but the generated RmvNaCh model provides larger coverage and includes DIIS3, additional DIIS4 regions, P-loop as well as DIIS6 and DIIIS6 regions (Figures 3 and 4B).

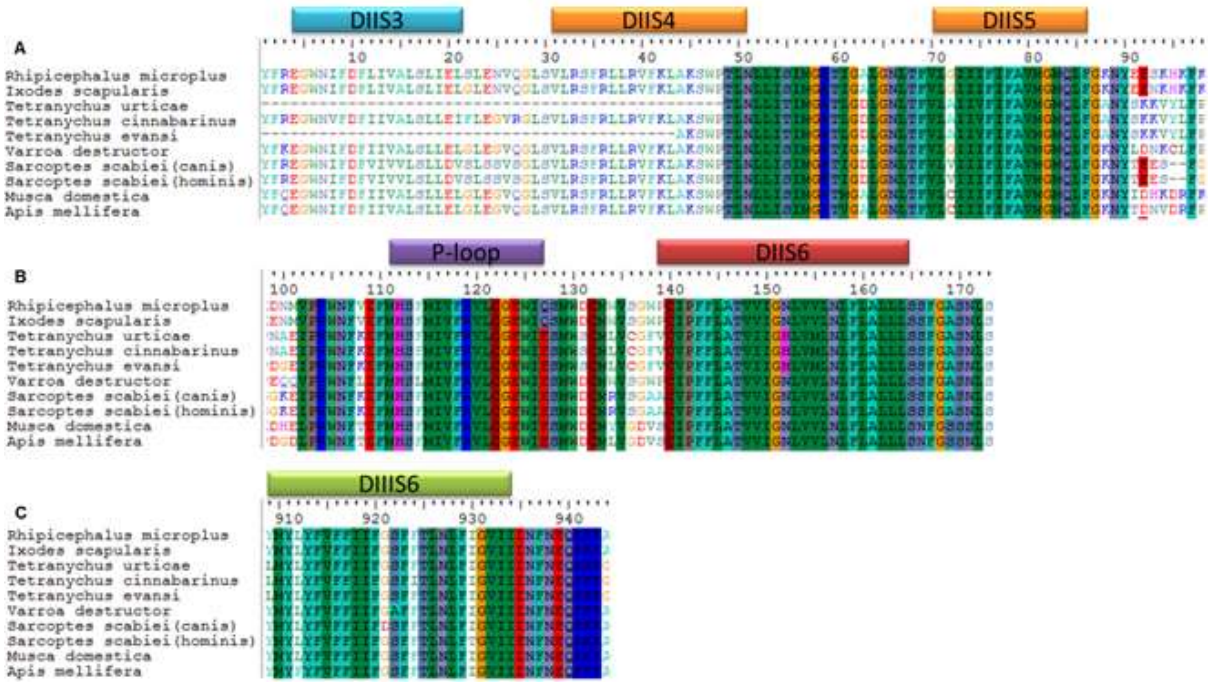

Figure 3: Multiple amino acid sequence alignment of the *R. microplus* voltage-gated sodium channel (RmvNaCh) with tick, mite and insect vNaChs. To illustrate the model coverage for the RmvNaCh model constructed. Sequence numbering done according to *R. microplus* amino acid numbers. A) Alignments for domain II S3 to S5 transmembrane helices. B) Alignments of domain II p-loop region and S6 transmembrane helix. C) Alignments of the domain III S6 transmembrane helix. *R. microplus* (cattle tick, AAD23600.2)*; Ixodes Scapularis* (black-legged tick, XP_002407119.1)*; Tetranychus urticae* (two-spotted spider mite, ADB92110.1)*; Tetranychus cinnabarinus* (carmine spider mite, ADD62494.1)*; Tetranychus evansi* (tomato red spider mite, ADK92428.1)*; Varroa destructor* (honeybee mite, AAP13992)*; Sarcoptes scabiei* (Canis) (canine scabies mite, ABL11237.1)*; Sarcoptes scabiei* (homonins) (human itch mite, ABB05337.3)*; Musca domestica* (common housefly, CAA65448)*; Apis mellifera* (European honeybee, NP_001159377.1).

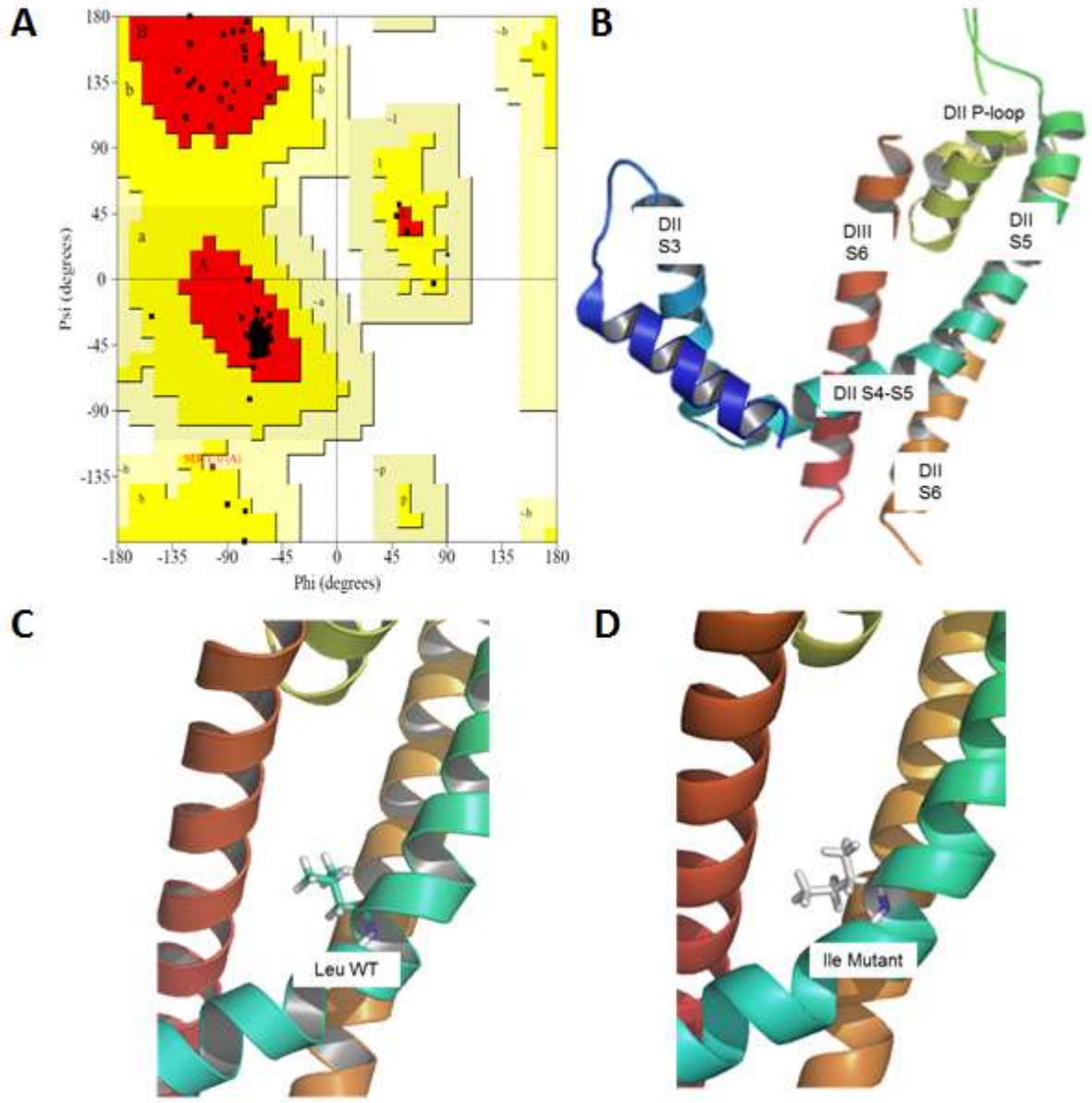

Figure 4: The constructed RmvNaCh model (partial model) showing the relevant pyrethroid binding domains and pyrethroid resistance associated SNP sites. A) The Ramachandran plot of the RmvNaCh model. The most favoured residue regions indicated in red, with additionally allowed regions in dark yellow and generously allowed regions in light yellow. B) The RmvNaCh model overview with domains constructed for domain II (DII) and domain III (DIII) S6. B) The pyrethroid resistance associated SNP site which is found in domain II S4-S5 linker region and the susceptible leucine (Leu WT) are indicated. C) The resistant mutant protein with isoleucine (Ile Mutant) instead of leucine.

Structural properties for the RmvNaCh model were analysed by means of a Ramachandran plot and found to be of a high quality with 95% of the residues in the most favoured regions of the plot (Figure 4A). This indicates that the core structure forming residues reside within experimentally determined states (bond lengths and bond angles of individual amino acids). As this is only a partial model, three more

domains are lacking. Inclusion of these domains would introduce more unstructured flexible loops (such as those between S5 and S6 helices), which most likely will reduce the Ramachandran score values. Figure 4C and D indicate the pyrethroid resistance associated SNP site which is found in domain II S4-S5 linker region, with the susceptible leucine and resistant isoleucine residues indicated respectively. A change in the amino acid side chain of the resistance substitution leads to a change in three dimensional space, which most likely impacts the electron density of this site.

Different cypermethrin stereoisomers were used for docking into the protein model in an attempt to provide insight into the biological mode underlying resistance. All eight stereoisomers were docked to the RmvNaCh model (both wild type (WT) and resistant mutant) and tabulated with the respective binding energies achieved for each docked pose (Figure 5). Docking of the 8 stereoisomers of cypermethrin using the resistant mutant protein model (Ile) as well as the susceptible wild type (Leu) model yielded a total of 144 docked poses. For each of the two proteins (WT and mutant), all 8 stereoisomers were docked (16 docking executions). For each docking execution, the top 9 docked poses were selected for further analyses. Three of the stereoisomers showed little to no difference in the docked poses generated when comparing the resistant mutant and susceptible wild type poses ((S)-cyano (1R, 3S), (R)-cyano (1S, 3S) and (R)-cyano (1R, 3S)). However, (R)-cyano (1R, 3S) did show a different orientation to all the other stereoisomers which does not appear to be consistent with O'Reilly et al. (2014). As the wild type and mutant poses differed in the remaining five stereoisomers it is evident that the resistance SNP site has an effect on drug docking.

Stereoisomer	Poses (same/different)	Binding energies (Kcal/mol) WT	Mutant	Figures WT (grey) and Mutant (red)
(S)-cyano (1S, 3S)	Different	-7.2	-6.7	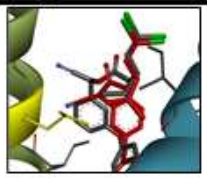
(S)-cyano (1S, 3R)	Different	-6.9	-6.6	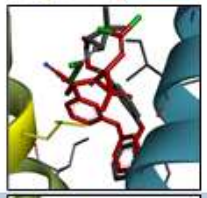
(S)-cyano (1R, 3S)	Same	-6.7	-7.0	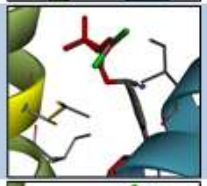
(S)-cyano (1R, 3R)	Different	-6.4	-6.5	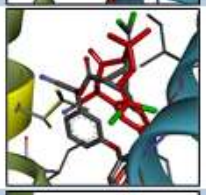
(R)-cyano (1S, 3S)	Same	-7.3	-7.2	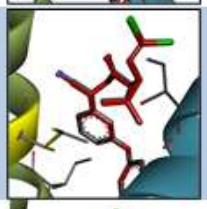
(R)-cyano (1S, 3R)	Different	-6.5	-6.4	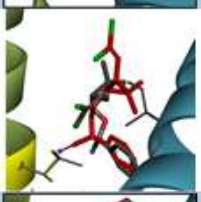
(R)-cyano (1R, 3S)	Same*	-6.8	-6.1	
(R)-cyano (1R, 3R)	Different	-6.1	-6.6	

Figure 5: Docked stereoisomers of cypermethrin to the RmvNaCh model. All eight stereoisomers of cypermethrin are shown, with their respective docked pose in the RmvNaCh model. The red structure indicates the resistant mutant docked pose and the grey structure represents the wild type/susceptible docked pose. The site indicated in yellow shows the resistance SNP loci. Binding energies for each pose is indicated in Kcal/mol.

Docked poses were also compared using dendrograms (calculated from RMSD values of each atom position) and arranged to show relatedness. Figure 6 shows the

following stereoisomers and how their docked positions relate to one another: (S)-cyano (1R, 3S), (R)-cyano (1R, 3S), (S)-cyano (1S, 3S), (R)-cyano (1S, 3S) and (R)-cyano (1S, 3R). It is clear that for (R)-cyano (1S, 3S) both the mutant and wild type docking generated the same pose and that this docked pose is closely related to that of (S)-cyano (1S, 3S) wild type. The (S)-cyano (1S, 3S) mutant docked position however seemed to generate a different pose, but still closely related. This suggests that for the cyano (1S, 3S) isomer the (S)/(R)-cyano organisation is the discriminatory factor between the wild type (susceptible) and mutant (resistant) orientation.

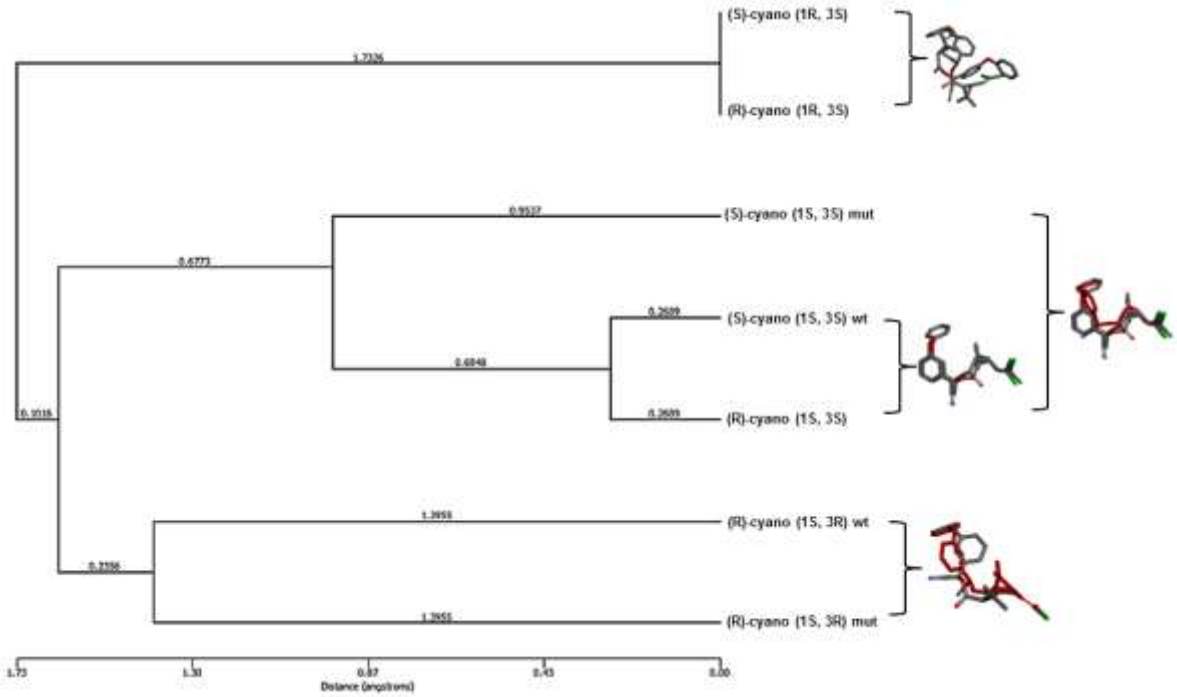

Figure 6: A refined dendrogram of the various docked cypermethrin stereoisomers on both the wild type (susceptible) and mutant (resistant) RmvNaCh model. The included poses are for (S)-cyano (1R, 3S), (R)-cyano (1R, 3S), (S)-cyano (1S, 3S), (R)-cyano (1S, 3S) and (R)-cyano (1S, 3R). The docked poses are overlaid. Stereoisomers (S)-cyano (1R, 3S) and (R)-cyano (1R, 3S) showed a 0.00 Å split.

Figure 7 gives a space filling view of the RmvNaCh model, showing the orientation of DIII S6 helix and the DII S4-S5 linker region in the closed conformation. The position of cypermethrin is indicated during the closed conformation. The S4-S5 linker region in horizontal conformation is twisted to a more vertical position during the opening of the pore via the S5 and S6 helices. Therefore when the DIII S6 helix opens, cypermethrin can slot in between the open section of the S6 helix with the S4-S5

linker and keep the pore open. Thus, if the resistant SNP residue (Ile) is present, then reduced stability of cypermethrin in this gorge could occur and entry to the interior of the protein might not be possible.

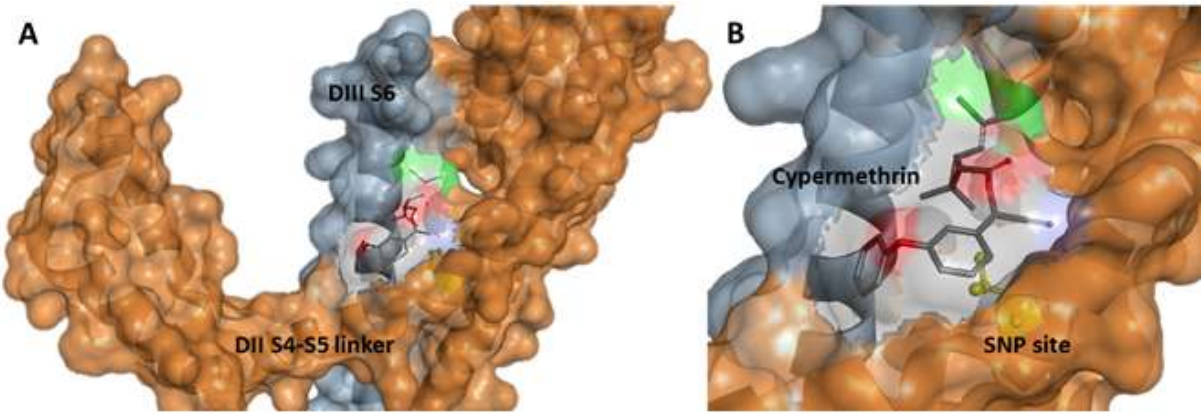

Figure 7: A space filling model of RmvNaCh with docked cypermethrin in closed channel conformation state. A) The space filling model shows cypermethrin as docked with the resistance associated SNP site in the closed conformation of the channel. Different domains of the channel are indicated. B) Closer view of cypermethrin as positioned with the SNP site indicated in yellow. *Though the docked pose generated was not different between the resistant mutant and susceptible wild type, the orientation of the pose was incorrect with regards to the other stereoisomers.

Discussion:

In South Africa the pyrethroid resistance-associated SNP marker, published by Morgan et al. (2009), for the voltage-gated sodium channel was found to occur as the homozygous-resistant genotype (AA) for majority of the *R. microplus* ticks. This observation coupled with a Tajima D value of <0 indicates that there is directional selection acting on the voltage-gated sodium channel. Selection pressure is driving the fixation of resistance alleles within the population, generating a lower average heterozygosity. It is therefore suggested that the L64I mutation within domain II of the sodium channel is a main pyrethroid resistance mechanism for *R. microplus* in South African tick populations, similar to global observed trends (Guerrero et al., 2012).

Sequence comparison between the *R. microplus* and *R. decoloratus* domain II sodium channel gene fragment showed no variation, however, a larger population of *R. decoloratus* samples will need to be sequenced to confirm this observation. It also appears that they share the same SNP that is linked to pyrethroid resistance in *R.*

microplus. This observation is expected as a number of farms sampled were co-infested with both *R. microplus* and *R. decoloratus*, where both species were exposed to pyrethroids. However, in *R. decoloratus* an excess of the heterozygous genotype within the voltage-gated sodium channel appears to be present. This indicates balancing selection, which acts to maintain the heterozygosity of the gene.

A comparison of the top ten pyrethroid resistant arthropods showed multiple resistant markers occurring across different species for the voltage-gated sodium channel (van Leeuwen et al., 2010). Regions that contain pyrethroid resistant SNP markers were: domain II S4-S5 linker region, domain II S5-S6 transmembrane helices, domain III S6 transmembrane helix and the domain IV S5-S6 transmembrane helices. None of the arthropods contained the exact same SNP in domain II S4-S5 linker region when compared to *R. microplus*, however, a pyrethroid resistance SNP occurring in domain III S6 (F1519I) of *R. microplus* is shared by *Tetranychus urticae* (van Leeuwen et al., 2010). This could indicate a shared homology for pyrethroid resistance markers across different species and may support the hypothesis of the domain II S4-S5 linker region SNP (L64I) as a resistance marker for *R. decoloratus*. As there is no published data for the full gene sequence of the voltage-gated sodium channel for *R. decoloratus*, a homology comparison cannot be done at this stage.

The initial frequency of resistance alleles must be taken into account when discussing resistance acquisition (Abbas et al., 2014). When dealing with the initial frequency of resistance alleles it must be noted that *R. microplus* is an invasive tick species while *R. decoloratus* is indigenous to Africa (De Clercq et al., 2012). This implies that *R. microplus* was introduced to Africa (subsequently South Africa) from global *R. microplus* tick populations for which pyrethroid resistance selection may have occurred in the countries of origin (Madder et al., 2011). Therefore, the initial frequency of resistant alleles may not have been equal for *R. microplus* and *R. decoloratus* populations, which may explain why *R. microplus* has acquired such a high level of homozygous resistance in South Africa. In addition, biological factors at play such as biotic and behavioural factors may also affect resistance acquisition (Abbas et al., 2014). Biotic factors would be generation times, offspring per generation and breeding patterns, while behavioural factors would include host range, mobility and migration (Abbas et al., 2014). *R. microplus* has a faster

generation time compared to *R. decoloratus* which may be the result for increased resistance acquisition (De Matos et al., 2009; Horak et al., 2009; Phalatsi et al., 2004). However, as previously mentioned, it takes approximately 18 months for both species to acquire resistance against pyrethroids (Rodriguez-Vivas et al., 2011). Further research is required to understand the differences in zygosity of this resistance allele for the two tick species. Lastly, there appears to be no sequence variation within domain II S4-5 linker region of the voltage-gated sodium channel between the different strains and the two species. This highly conserved region seems to respond to pyrethroid selection pressure in the same manner across different strains and the two closely related species. This suggests that a single diagnostic approach may be effective.

The voltage-gated sodium channel model (RmvNaCh)

Previous attempts to build a model for *R. microplus* utilised structures from potassium-gated channels (O' Reilly et al., 2014). The aim of this study set out to construct a higher quality model with more sequence coverage in amino acid sequence alignments, thus producing a higher coverage model. Alignments of *R. microplus* voltage-gated sodium channel (AF134216.2) with template proteins showed very little coverage through BLAST analysis. The entire first domain (DI) of the sequence is absent for *R. microplus*.

Four crystal structure templates where assessed to model the respective domains. Since none of the templates achieve full coverage of all the domains, each domain was used to match with separate template structures. The resistance SNP which occurs in domain II received priority. The four templates identified where: 4DXW (prokaryote vNaCh: all four domains), 3RVY (1 domain coverage), 4EKW (1 domain coverage), 3RWO (1 domain coverage) and 4BGN (1 domain coverage). Crystal template 4DXW showed more coverage than the others and included domain II (priority) and sections of domain III (enough for the formation of a drug binding pocket). The other templates only covered a single domain. The 4BGN template was suitable for construction of domain II (DII), however this structure was derived from cryo-electron microscopy effecting resolution. Template 4DXW showed the highest maximum sequence identity of 30.2% for domain II (including domain III S6). This

would include all the hypothesised residues present during binding of pyrethroids in the drug pocket (O' Reilly et al., 2014).

The mechanism of action proposed for pyrethroids is that the acaricide binds to the open conformation of voltage-gated sodium channels and renders them open for longer, resulting in a larger influx of Na^+ into the cell (larger repolarization of cells) and thus aperiodic discharge of neurons (Lees and Bowman, 2007). Since the voltage sensor and directly adjacent hinge motif (S4-S5 linker) are responsible for the opening and closing of the pore, pyrethroid binding is thought to occur within this region. When taking into account the localization of known resistance SNPs for this channel in different arthropods, mutations in this linker region is frequently observed (van Leeuwen et al., 2010). Therefore SNP regions within the DII S4-S5 linker region were included as part of the search space/docking sphere when docking was performed.

Three of the stereoisomers showed little to no difference in the docked poses generated between the resistant mutant and the susceptible wild type poses ((S)-cyano (1R, 3S), (R)-cyano (1S, 3S) and (R)-cyano (1R, 3S)). For the rest of the stereoisomers the mutant SNP did produce different docking results. Analysis of the different docked poses through use of a dendrogram (Figure 6) highlighted (R)-cyano (1S, 3S), which showed the same docked pose for both the wild type and resistant mutant. The (R)-cyano (1S, 3S) stereoisomer also shows close relations to (S)-cyano (1S, 3S) wild type pose and a further relation to (S)-cyano (1S, 3S) mutant pose (Figure 6). Two factors are relevant here; the first is the effect of (R/S)-cyano stereochemistry and secondly the effect of the mutant or wild type SNP. For the (R)-cyano stereochemistry it is not evident that the SNP site had an impact on the docked pose generated. However, for the (S)-cyano stereochemistry the SNP site affect the docked pose showing a clear difference between wild type and mutant. Also the mutant docked pose deviates further from the wild type (S)-cyano (1S, 3S) and the (R)-cyano (1S, 3S), Indicating that (R)-cyano (1S, 3S) binding is effective in both mutant and wild type. We therefore hypothesis that the (R)-cyano (1S, 3S) stereoisomer will be effective in both pyrethroid resistant and susceptible *R. microplus*. However, further investigation through means of bioassays is required to validate these findings.

In silico predictive modelling plays a vital role in future drug docking studies for the discovery of novel and improved acaricides. These improved control strategies will be largely beneficial if they can be applied to both *Rhipicephalus* species.

Acknowledgements

This study was funded by Zoetis Pty. Ltd South Africa, the National Research Foundation Technology and Human Resources for Industry Programme (grant number TP 12082911252). A special thanks to Dr. Annette-Christie Barnard for critical reading of this manuscript.

References

Abbas, R.Z., Arfan, M., Colwell, D.D., Gilleard, J., Iqbal, Z., 2014. Acaricide resistance in cattle ticks and approaches to its management : The state of play. Vet. Parasitol. 203, 6–20.

Aguirre, J., Sobrino, A., Santamar´ıa, M., Aburto, A., Roman, S., Hernandez, M., 1986. Resistancia de garrapatas en Mexico.Seminario Internacional de Parasitologia Animal, Cuernavaca,Morelos, Mexico, 8–10 September 1986, ed by Caravazzai AH and Garcia Z. 282–306.

Baffi, M.A., De Souza, G.R.L., Vieira, C.U., 2007. Identification of point mutations in putative carboxylesterase and their association with acaricide resistance in *Rhipicephalus (Boophilus) microplus* (Acari: Ixodidae). Vet. Parasitol. 148, 301–309.

Baron, S., van der Merwe, N.A., Madder, M., Maritz-Olivier, C., 2015. SNP analysis infers that recombination is involved in the evolution of amitraz resistance in *Rhipicephalus microplus*. PLoS One 10, 1–20.

De Clercq, E.M., Vanwambeke, S.O., Sungirai, M., Adehan, S., Lokossou, R., Madder, M., 2012. *Rhipicephalus microplus* , a country-wide survey in Benin. Exp. Appl. Acarol. 441–452.

De Matos, C., Sitoe, C., Neves, L., Nothling, J.O., Horak, I.G., 2009. The comparative prevalence of five ixodid tick species infesting cattle and goats in Maputo Province, Mozambique. Onderstepoort J Vet Res 76, 201–208.

Guerrero, F.D., Davey, R.B., Miller, R.J., 2001. Use of an Allele-Specific Polymerase Chain Reaction Assay to Genotype Pyrethroid Resistant Strains of *Boophilus microplus* (Acari: Ixodidae). J. Med. Entomol. 38, 44–50.

Guerrero, F.D., Lovis, L., Martins, J.R., 2012. Acaricide resistance mechanisms in *Rhipicephalus (Boophilus) microplus*. Rev Bras Parasitol Vet. 21, 1–6.

Hall, T., 1999. BioEdit: Biological sequence alignment editor for Win95/98/NT/2K/XP. Nucl Acids Symp Ser 41, 95–98.

He, H., Chen, A.C., Davey, R.B., Ivie, G.W., George, J.E., 1999. Identification of a point mutation in the para-type sodium channel gene from a pyrethroid-resistant cattle tick. Biochem Bioph Res Co. 261, 558–561.

Horak, I.G., Nyangiwe, N., De Matos, C., Neves, L., 2009. Species composition and geographic distribution of ticks infesting cattle, goats and dogs in a temperate and in a subtropical region of south-east Africa. Onderstepoort J. Vet. Res. 76, 263–276.

Jonsson, N.N., 2006. The productivity effects of cattle tick (*Boophilus microplus*) infestation on cattle, with particular reference to Bos indicus cattle and their crosses. Vet. Parasitol. 137, 1–10.

Jonsson, N.N., Cutullè, C., Corley, S.W., Seddon, J.M., 2010. Identification of a mutation in the para-sodium channel gene of the cattle tick *Rhipicephalus microplus* associated with resistance to flumethrin but not to cypermethrin. Int J Parasitol. 40, 1659–1664.

Jonsson, N.N., Davis, R., De Witt, M., 2001. An estimate of the economic effects of cattle tick (*Boophilus microplus*) infestation on Queensland dairy farms. Aust. Veterninary J. 79, 826–831.

Katoh, Standley, 2013. MAFFT multiple sequence alignment software version 7: improvements in performance and usability. Mol Biol Evol. 30, 772–780.

Lees, K., Bowman, A.S., 2007. Tick neurobiology: recent advances and the post-genomic era. Invertebr Neurosci. 7, 183–198.

Lempereur, L., Geysen, D., Madder, M., 2010. Development and validation of a PCR–RFLP test to identify African *Rhipicephalus* (*Boophilus*) ticks. Acta Trop. 114, 55–58.

Madder, M., Horak, I.G., 2010. Tick Photodatabase. Tick Species.

Madder, M., Thys, E., Achi, L., Toure´, A., De Deken, R., 2011. *Rhipicephalus* (*Boophilus*) *microplus*: a most successful invasive tick species in West-Africa. Exp. Appl. Acarol. 53, 139–145.

Miller, R.J., Davey, R.J., George, J.E., 1999. Characterization of pyrethroid resistance and susceptibility to coumaphos in Mexican *Boophilus microplus* (Acari: Ixodidae). J. Med. Entomol. 36, 533–538.

Morgan, J.A.T., Corley, S.W., Jackson, L.A., Lew-Tabor, A.E., Moolhuijzen, P.M., Jonsson, N.N., 2009. Identification of a mutation in the para-sodium channel

gene of the cattle tick *Rhipicephalus* (*Boophilus*) *microplus* associated with resistance to synthetic pyrethroid acaricides. Int J Parasitol. 39, 775–779.

O' Reilly, A.O., Williamson, M.S., Gonz, J., Turberg, A., Field, L.M., Wallace, B.A., Davies, T.G.E., 2014. Predictive 3D modelling of the interactions of pyrethroids with the voltage-gated sodium. Pest 70, 369–377. doi:10.1002/ps.3561

Phalatsi, M.S., Fourie, L.J., Horak, I.G., 2004. Larval biology of *Rhipicephalus* (*Boophilus*) *decoloratus* (Acarina: Ixodidae) in Free State Province, South Africa. Onderstepoort J Vet Res 71, 327–331.

Pruett, J.H., Guerrero, F.D., Hernandez, R., 2002. Isolation and Identification of an Esterase from a Mexican Strain of *Boophilus microplus* (Acari: Ixodidae). J. Econ. Entomol. 95, 1001–1007.

Rodriguez-Vivas, R.I., Trees, A.J., Rosado-Aguilar, J.A., Villegas-Perez, S.L., Hodgkinson, J.E., 2011. Evolution of acaricide resistance: Phenotypic and genotypic changes in field populations of *Rhipicephalus* (*Boophilus*) *microplus* in response to pyrethroid selection pressure. Int J Parasitol 41, 895–903.

Soderlund, D.M., Knipple, D.C., 2003. The molecular biology of knockdown resistance to pyrethroid insecticides. Insect Biochem Mol Biol 33, 563–577.

Tajima, F., 1989. Statistical methods to test for nucleotide mutation hypothesis by DNA polymorphism. Genetics 123, 585–595.

Tamura, K., Peterson, D., Peterson, N., Stecher, G., Nei, M., Kumar, S. (2011)., 2011. MEGA5: Molecular Evolutionary Genetics Analysis using Maximum Likelihood, Evolutionary Distance, and Maximum Parsimony Methods. Mol Biol Evol 10, 2731–2739.

Trott, O., Olson, A.J., 2009. Software News and Update AutoDock Vina : Improving the Speed and Accuracy of Docking with a New Scoring Function , Efficient Optimization , and Multithreading.

Van Leeuwen, T., Vontas, J., Tsagkarakou, A., Dermauw, W., Tirry, L., 2010. Acaricide resistance mechanisms in the two-spotted spider mite *Tetranychus urticae* and other important Acari : A review. Insect Biochem. Mol. Biol. 40, 563–572.

Vargas, M.S., Sanchez, H.F., Vazquez, Z.G., 2002. First case reported of amitraz resistance in the cattle tick *Boophilus microplus* in Mexico. Téc Pecu Méx. 40, 81–92.

Walker, A.R., Bouattour, A., et al, 2003. Ticks of Domestic Animals in Africa: a Guide to Identification of Species. Edinburgh, Biosci. Reports.

Supplementary material

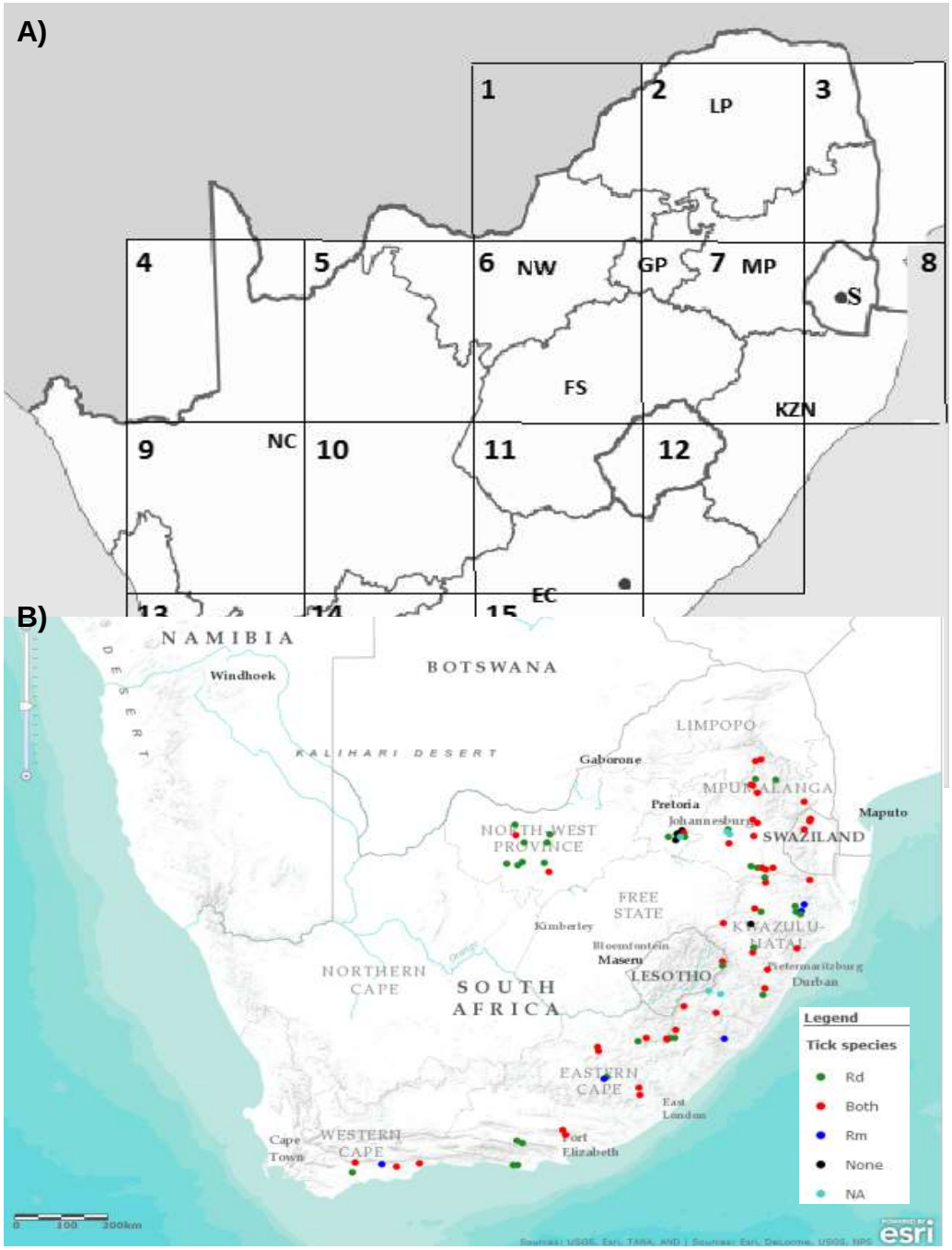

Figure S1.Sample collection points for ticks across South Africa. A) Ticks from each farm were placed into subpopulations (1-15) depending on the region (Grid block) from which they were collected (Baron et al. 2015). LP – Limpopo, NW – North West, MP – Mpumalanga, NC – Northern Cape, FS – Free State, GP – Gauteng, KZN – Kwa-Zulu Natal, WC – Western Cape, EC – Eastern Cape and S – Swaziland. B) Sampling points of cattle farms throughout South Africa in high and medium cattle density areas. Rd – *Rhipicephalus decoloratus*, Rm – *Rhipicephalus microplus*.

Table S1.Tick collection inventory for *Rhipicephalus microplus* across sample points in South Africa.

Grid Block	Farm number	Sample number	Allele Status	Grid Block	Farm number	Sample number	Allele Status
2	44	44.2MF	RR	8	51	51.1MF	SS
	46	46.2MF	RR			51.2MF	SS
		46.3MF	RR			51.3MF	SS
7	20	20.1MF	RR			51.4MF	SS
		20.3MF	RR			51.5MF	SS
	26	26.1MF	RS		66	66.1MF	RR
		26.6MF	RS			66.2MF	RR
		26.7MF	SS			66.5MF	RR
		26.8MF	RR			67.1MF	RR
	47	47.2MF	RR			67.2MF	RR
	54	54.2MF	RR		67	67.3MF	RR
		54.7MF	RR			67.4MF	RR
		54.10MF	RR			67.5MF	RR
	73	73.1MF	RR		69	69.3MF	RR
		73.2MF	RR	12	7	7.5MF	SS
		73.3MF	RR		37	37.1MF	SS
		73.4MF	RR			37.2MF	SS
		73.5MF	RR		41	41.2MF	RS
		73.7MF	RR			41.12MF	RR
		73.8MF	RR			41.13MF	RR
	86	86.2MF	RR		62	62.1MF	RR
		86.4MF	RS			62.2MF	RR
		86.6MF	RR			62.4MF	SS
		86.7MF	RR			62.5MF	SS
	45	45.1MM	SS		65	65.1MF	RR
		45.4MM	SS			65.2MF	RR
		45.5MM	SS			70.1MF	RR
8	50	50.2MF	RR		70	70.3MF	RR
		50.3MF	RR			70.2MF	RR
		50.4MF	RS	Overall Allele Status		RR	58.8%
		50.5MF	SS			RS	8.8%
						SS	32.4%

Table S2.Tick collection inventory for *Rhipicephalus decoloratus* across sample points in South Africa.

Grid Block	Farm number	Sample number	Allele Status
2	44	44.1	RR
	46	46.3	RS
	71	71.1	RS
		71.2	RS
		71.5	RS
	81	81.1	RS
		81.2	RS
		81.3	RS
		81.4	RS
		81.5	RS
		81.7	RS
		81.8	RS
		81.9	RS
		81.10	RR
	98	98.1	RR
		98.2	RS
		98.3	RS
		98.4	RS
		98.5	RR
	102	102.1	RS
		102.4	RS
		102.5	RS
		102.6	RS
		102.8	RS
		102.9	RR
		102.10	RS
7	20	20.1	RS
		20.2	SS
		20.4	RS
		20.5	RS
	23	23.1	RS
	45	45.1	RS
	54	54.7	RR
	86	86.1	RS
		86.2	RR
8	66	66.10	RS
	67	67.2	SS
		67.3	RS
	68	68.2	RR
		68.3	RR
	69	69.2	RS
		69.3	RS
12	49	49.5	RR
	58	58.2	RS
Overall Allele Status		RR	22%
		RS	73%
		SS	5%